Chapter 5

Screening a compound library that targets the NF-κB pathway in human T cells

5.1 Introduction

The assay developed to measure degranulation and killing simultaneously was successfully used for a small screen in mCTL in chapter 4. The work in this chapter aimed to 1) test whether this assay also works in hCTL, as a more medically relevant cell type, and 2) to test the extent to which the combined degranulation and killing assay can be scaled.

In chapter 3, CRISPR was used to target *Munc13-4*, *Rab27a* and the gene encoding perforin (*Prf1*) in mCTL and the resulting samples were used to validate the newly developed combined degranulation and killing assay. Since I had not yet set up the CRISPR technology in hCTL, I instead used cells derived from FHL2 and FHL3 patients to address point 1. FHL2 is caused by mutations in *PRF1*, and FHL3 is associated with mutations in *MUNC13-4*. Both of these genes are crucial for CTL function as demonstrated by data shown in chapter 3 and the literature (Crozat et al., 2007; Feldmann et al., 2003; Kägi et al., 1994a; Stepp et al., 1999).

To test the scalability of the assay, I used a chemical compound library targeting the NF-κB signalling pathway obtained from Medchem express. The combined degranulation and killing assay, performed in a 96 well format, was reasoned to be easily adaptable for screening dozens of compounds. The NF-κB compound library consisted of 64 drugs, and allowed me to test the scalability of the combined degranulation and killing assay while

simultaneously asking whether NF-κB has a direct role in CTL killing.

The canonical NF-κB signalling pathway is known to be activated in response to TCR recognition of its cognate antigen in the context of MHC class I. TCR signalling and CD28 co-stimulatory signals trigger activation of PKCθ and its recruitment to the IS (Oh and Ghosh, 2013; Paul and Schaefer, 2013). PKCθ has been shown to phosphorylate CARMA1, and phosphorylated CARMA1 can bind to BCL10 and MALT1 (Schulze-Luehrmann and Ghosh, 2006; Vallabhapurapu and Karin, 2009). MALT1 and BLC10 are thought to be polyubiquitinated by TRAF6 (Paul and Schaefer, 2013), resulting in recruitment of the IκB kinase (IKK) complex, consisting of IKKα, IKKβ and IKKγ, via the polyubiquitination binding motif of IKKγ (Paul and Schaefer, 2013). Subsequently, IKKγ and IKKβ are activated by polyubiquitination and phosphorylation, respectively. Activated IKKβ phosphorylates the inhibitor of κB (IκB), which triggers ubiquitination and degradation of IκB via the 26S proteasome (Paul and Schaefer, 2013; Vallabhapurapu and Karin, 2009).

The NF-κB family of transcription factors consists of p105/p50 (NFkB1), p100/p52 (NFkB2), p65 (RelA), RelB and c-Rel (Paul and Schaefer, 2013; Vallabhapurapu and Karin, 2009). They share a Rel homology domain that is important for DNA binding and dimerisation (Oh and Ghosh, 2013; Vallabhapurapu and Karin, 2009). Under basal conditions, NF-κB is retained in the cytoplasm as inactive heterodimers or homodimers bound by the inhibitor of κB. TCR-mediated degradation of IκB, as outlined above, allows NF-κB dimers to translocate into the nucleus and regulate transcription of their target genes (Vallabhapurapu and Karin, 2009).

In the nucleus, NF-κB transcription factors bind to promoters that contain κB binding sites. One crucial NF-κB target gene is the gene encoding IκBα, thereby ensuring a negative feedback mechanism to terminate NF-κB signalling (Vallabhapurapu and Karin, 2009). NF-κB is reported to activate expression of over 150 target genes, including cytokines, chemokines and adhesion molecules (Pahl, 1999). NF-κB target genes are important for T cell activation, proliferation, differentiation and survival (Schulze-Luehrmann and Ghosh, 2006; Vallabhapurapu and Karin, 2009). It is clear that the NF-κB signalling pathway is crucial for T cell function, but less is known about its importance for CTL killing specifically. The NF-κB drug library was used to investigate the role of NF-κB in degranulation of CTLs and their killing.

5.1.1 Chapter aims

- Test the combined degranulation and killing assay in hCTL using FHL2 and FHL3 patient samples.
- Investigate the scalability of the assay using a NF-κB compound library.
- Follow up promising hits to elucidate their mechanism of action.

5.2 Results

5.2.1 Testing the combined degranulation and killing assay using patient-derived CTL

The combined degranulation and killing assay was tested in hCTL using cells derived from FHL3 patients (carrying mutations in *MUNC13-4*) and FHL2 patients (carrying mutations in *PRF1*). The exact mutations of all patients are outlined in chapter 2, Table 2.2. hCTL derived from FHL3 patients significantly degranulated less (n=3, $p<0.0001$, unpaired t-test with Welch's correction) and killed target cells less efficiently (n=3, $p<0.01$, unpaired t-test with Welch's correction) than hCTL derived from HDs (Figure 5.1A,B). The killing phenotype was confirmed for every patient using the Incucyte killing assay (Figure 5.1C-E). In agreement with the phenotype observed, WB showed that less MUNC13-4 protein was expressed in patient-derived cells than in cells derived from HDs (Figure 5.1F).

Cells derived from FHL2 patients did not show a defect in degranulation (Figure 5.2A), but showed a significant decrease in the ability to kill target cells (n=4, $p<0.0001$, unpaired t-test with Welch's correction) (Figure 5.2B). Again, the killing phenotype was confirmed using the Incucyte killing assay (Figure 5.2C-F). WB for perforin showed that less protein was expressed in patient-derived cells than in cells derived from HDs (Figure 5.2G). Interestingly, the perforin antibody recognised two bands in lysates derived from patient 6981 and patient 3026 (Figure 5.2G). These bands were of a higher molecular weight than the banding pattern produced in samples derived from 5 different HDs. This suggested that while the mutations in patients 6981 and 3026 did not cause a complete loss of perforin, they still resulted in impaired protein function. In summary, the patient results demonstrated that the combined degranulation and killing assay can be used to reliably identify hCTLs with a defect in killing, degranulation, or both.

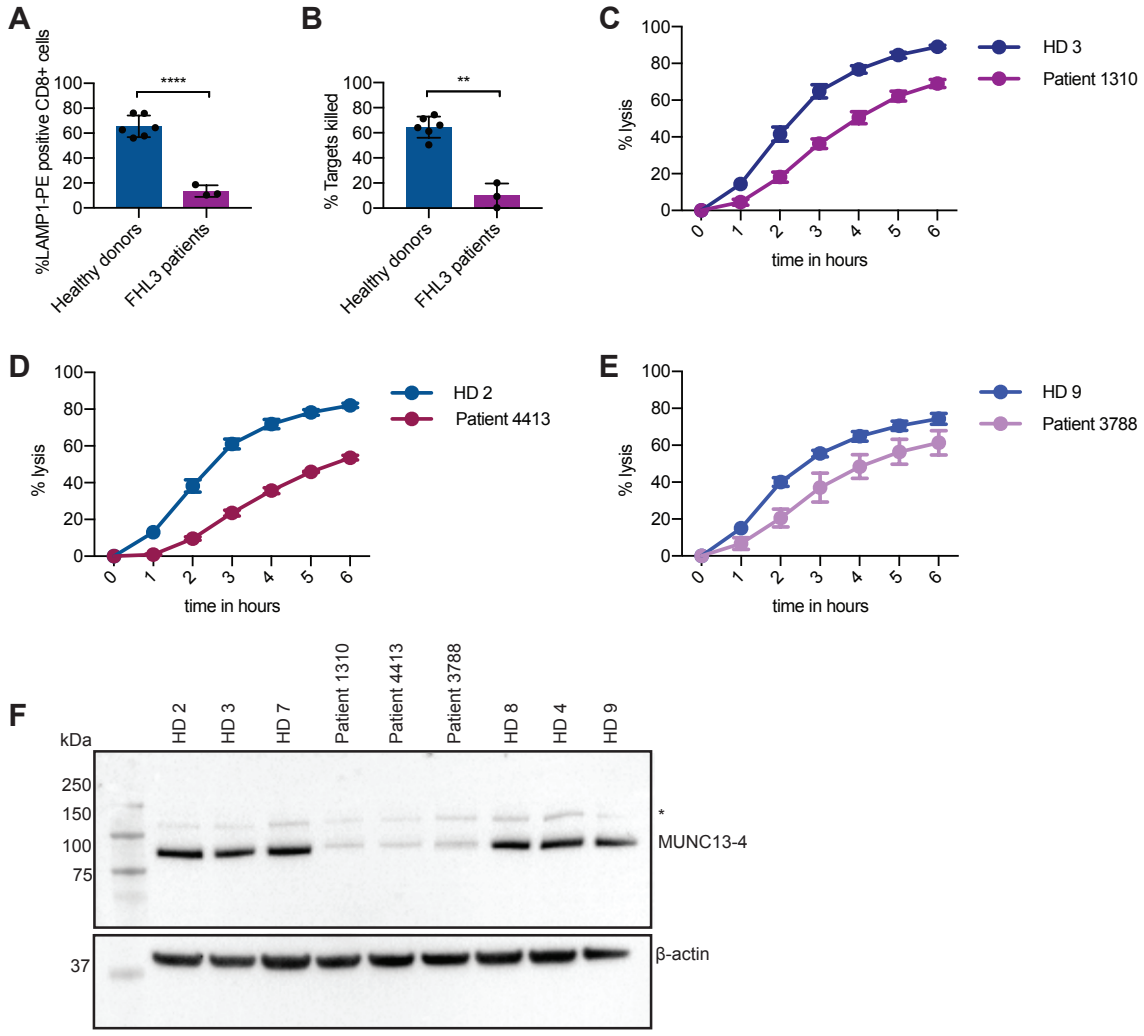

Fig. 5.1 ***Decreased degranulation and killing in cells derived from FHL3 patients.*** ***A*** *The degranulation and* ***B*** *killing readout of the combined degranulation and killing assays were analysed following the gating strategy and calculations described in chapter 2, section 2.5.2. CTLs were derived from three independent FHL3 patients and compared to CTLs derived from 6 independent HDs. All samples were purified to isolate CD8 cells. E:T ratio = 2.5:1, assay duration = 180 min. Each data point is the average of 2-4 technical repeats. **p<0.01, ****p<0.0001 as calculated by unpaired t-test with Welch's correction. Bar graphs show the mean ± SD.* ***C*** *Incucyte killing assay showing % lysis of red P815 target cells in the presence of αCD3 and HD 3 or patient 1310,* ***D*** *HD 2 or patient 4413 and* ***E*** *HD 9 or patient 3788. E:T = 2.5:1. Each datapoint is an average of 3-4 technical repeats and the error bars show the SD.* ***F*** *WB showing MUNC13-4 and β-actin (loading control) protein expression in CTL derived from the indicated HDs and patients. HD = healthy donor, SD = standard deviation, us = unspecific, FHL = familial hemophagocytic lymphohistiocytosis. * = potentially non-specific band.*

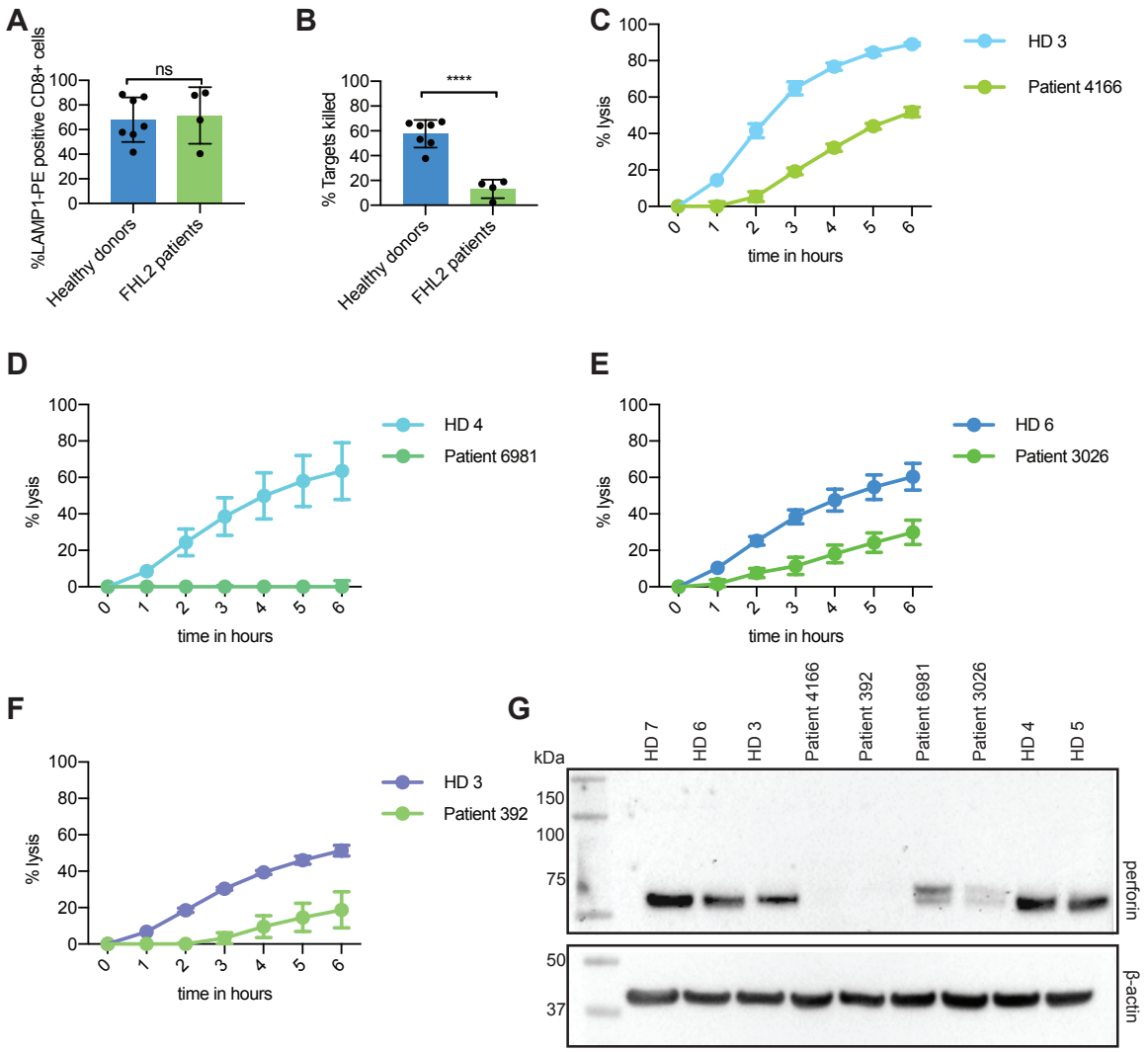

Fig. 5.2 ***CTLs derived from FHL2 patients showed a killing defect.*** ***A*** *The degranulation and* ***B*** *killing readout of the combined degranulation and killing assays were analysed following the gating strategy and calculations described in chapter 2, section 2.5.2. CTLs were derived from four independent FHL2 patients and compared to CTLs derived from 7 independent HDs. All samples were purified to isolate CD8 cells. E:T ratio = 2.5:1, assay duration = 180 min. Each data point is the average of 2-4 technical repeats. ****p<0.0001 as calculated by unpaired t-test with Welch's correction. Bar graphs show the mean ± SD.* ***C*** *Incucyte killing assay showing % lysis of red P815 target cells in the presence of αCD3 and HD 3 or patient 4166,* ***D*** *HD 4 or patient 6981,* ***E*** *HD 6 or patient 3026 and* ***F*** *HD 3 or patient 392. E:T = 2.5:1. Each datapoint is an average of 3-4 technical repeats and the error bars show the SD.* ***G*** *WB showing perforin and β-actin (loading control) protein expression in CTL derived from the indicated HDs and patients. HD = healthy donor, SD = standard deviation, FHL = familial hemophagocytic lymphohistiocytosis.*

5.2.2 Compound library toxicity testing

So far, the combined degranulation and killing assay had been used to screen just over a dozen genetic targets (chapter 4). To test the scalability of this assay, I used a drug library of 64 compounds reported to target the NF-κB signalling pathway. Figure 5.3 shows the composition of this library in terms of molecular targets. Some molecular targets, such as MALT1, IKK and NF-κB, are direct components of the NF-κB signalling cascade downstream of the TCR, as outlined in section 5.1. The RIP kinase is also implicated in activation of the NF-κB signalling pathway (He and Wang, 2018), therefore inhibitors of RIP kinase should inhibit NF-κB function. In contrast members of the PPAR family have been shown to inhibit NF-κB (reviewed by Ricote and Glass (2007)). NRF2, regulated by the protein KEAP1, was shown to inhibit NF-κB, and NF-κB activity is enhanced when NRF2 levels are decreased (reviewed in Wardyn et al. (2015)).

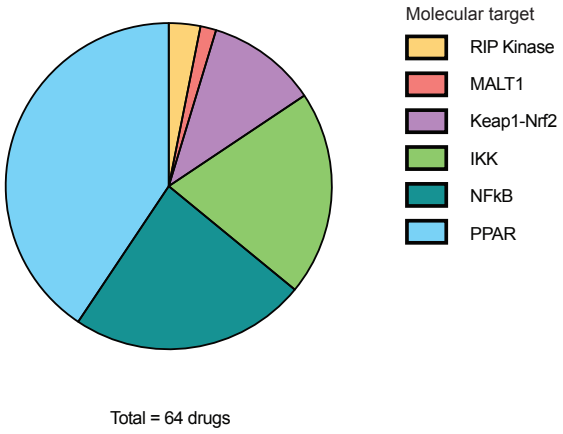

Fig. 5.3 ***Overview of molecular targets of the NF-κB signalling compound library.*** *Piechart showing the molecular targets of the 64 compounds contained in the library obtained from Medchem express. The library contained activators as well as inhibitors. 2 drugs are reported to target RIP kinase, 1 drug is reported to target MALT1, 7 drugs target Keap1-Nrf2, 13 drugs target IKK, 15 drugs target NF-κB and 26 drugs target PPAR. This information was provided by Medchem express.*

For simplicity, the drugs were labelled 1-64 according to the order in which they were supplied. The Celltitre assay (see chapter 2, section 2.8) was used as a toxicity test to determine whether the drugs were toxic to hCTL after overnight treatment with a range of concentrations (Figure 5.4). Initially, I tested the sensitivity of the Celltitre assay, in which absorbance at 490 nm should correspond to the amount of metabolically active cells. I seeded

a range of hCTL per well and measured the absorbance after 4 h incubation with the Celltitre reagents. This clearly showed that absorbance decreased as the number of cells decreased (Figure 5.4A), indicating that this assay could be used to test for toxicity in response to drug treatment.

The highest concentration to be tested was set to 25 μM. This upper threshold was in part based on the EC50/IC50 information provided by the supplier of the compound library, although this information was not available for all 64 compounds. Additionally, using drugs at a maximum of 25 μM meant that the percentage of DMSO to be added to the vehicle control could be kept at, or below, 0.25%. The Celltitre assay was used to show that treating cells with 0.25% DMSO for 24 h did not show toxic effects (Figure 5.4B).

Next, drugs were tested for toxic effects at concentrations between 0.1 μM and 25 μM, achieved by performing serial three-fold dilutions. Corresponding DMSO controls were included on every plate. The change in absorbance in response to treatment with drugs at various concentrations was plotted as a curve (example plots shown in Figure 5.4C-F). This was used to visually determine the highest concentrations that were not toxic to hCTLs over a 24 h time period. To give an example, drug 4 only showed toxic effects above a concentration of 0.9 μM (Figure 5.4C). Therefore 0.9 μM was chosen as the highest non-toxic concentration for drug 4. For drugs that did not show a toxic effect, such as drug 22, the highest concentration tested, 25 μM, was chosen as the concentration to use in the functional assay (Figure 5.4F). The Table C.1 (Appendix C) outlines the highest non-toxic concentration for all drugs in the library, determined as described above, as well as their official names and their reported molecular target. The highest non-toxic concentration was the concentration used for each drug in all further assays.

5.2.3 Compound screen using the combined degranulation and killing assay

hCTL were treated with the highest non-toxic concentration overnight before functional testing using the combined degranulation and killing assay. The screen was performed across seven 96-well plates using cells from the same HD used for toxicity testing at day 13-15 post in vitro stimulation. Up to 12 samples fit per plate when testing each condition in duplicate. In addition to the stimulated experimental samples (containing hCTL + P815s + αCD3), I also included unstimulated controls (hCTL + P815s) as well as hCTL and P815s on their

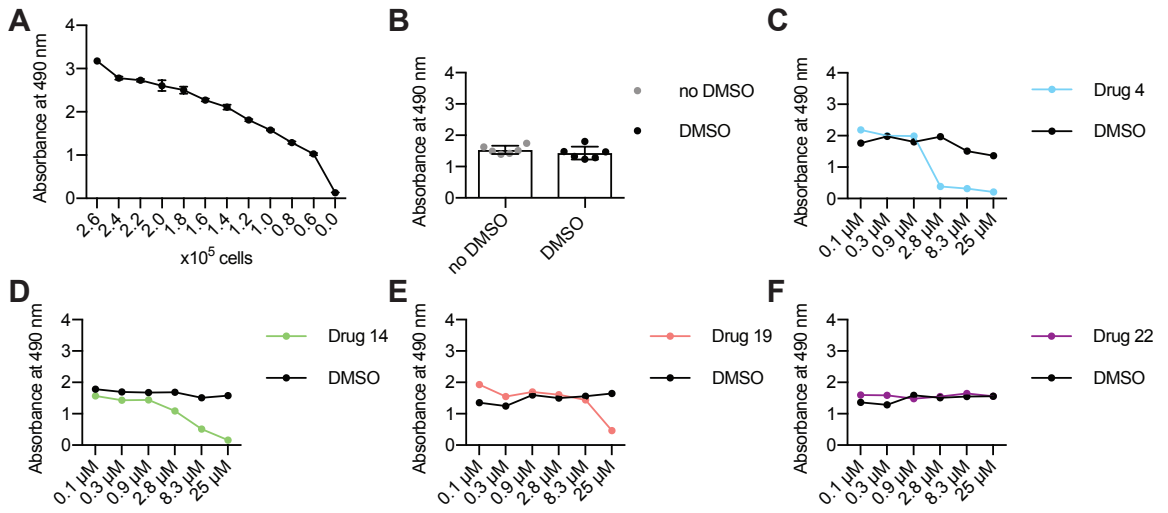

Fig. 5.4 ***Testing the toxic effect of compounds on hCTL. A*** *The indicated number of cells were seeded in each well of a 96 well plate and incubated with Celltitre reagent for 4 h. Absorbance at 490 nm was measured.* ***B*** *Cells were treated with the amount of DMSO equivalent to treatment with 25 µM drugs. Cell viability after 24 h treatment was compared to control cells that were not treated with DMSO. The Celltitre reagent was added 4 h before the end of the 24 h incubation period. Absorbance at 490 nm was measured, n=6 independent experiments. Bar graphs show the mean ± SD.* ***C-F*** *125,000 hCTL were seeded per well in a 96 well plate and treated with drugs at the indicated concentrations for approximately 24 h. Examples for drug 4, 14, 19 and 22 are shown. The assay readout was used to determine the highest non-toxic concentration for every drug in the library.*

own treated with drugs, in order to be able to detect any effects the drugs might have on these cell types. The degranulation readout from the screen is shown in Figure 5.5 and the killing readout is shown in Figure 5.6. Drug 37 had to be excluded in the killing assay analysis, as it appeared to be toxic to P815 target cells over the course of the 3 h assay, therefore affecting the killing assay result for this sample.

While there were many drugs that seemed to decrease degranulation or killing, there were no drugs that substantially increased degranulation or killing. Only drugs that reduced degranulation or killing by more than 50% in comparison to the appropriate DMSO control were chosen for follow up analysis. Drug 26 was therefore classified as a potential hit according to the degranulation aspect of the screen (Figure 5.5), and drugs 4, 13, 19, 24, 30 were classified as potential hits according to the killing aspect of the screen (Figure 5.6). Drug 14 was not classified as a potential hit due to large variability between technical repeats.

It is likely that some drugs that do have an effect on degranulation or killing did not pass these stringent cut-off criteria. For example, drug 30 (46% decrease in degranulation) and drug 4 (48% decrease in degranulation) were close to passing the degranulation threshold, but encouragingly they were also picked up as potential hits in the killing aspect of the screen. The aim of this screen was not to identify and characterise every single promising drug, but to investigate the possibility to use the combined degranulation and killing assay for a mid-size screen, while focusing on the most promising hits that could be useful to further investigate the importance of NF-κB in the CTL killing process.

5.2.4 Testing the reproducibility of potential hits

To test whether the effects of drug 4, 13, 19, 24, 26 and 30 in the combined degranulation and killing assay were reproducible, hCTLs derived from independent HDs were treated with drugs at the same concentrations previously used (Figure 5.7). Each drug treatment is connected to its corresponding DMSO control treatment, which was performed simultaneously on the same cells (Figure 5.7). Not all hits were reproducible, indicating that some hits were false positives. Additionally, as the screen was performed on cells derived from one HD, some donor-to-donor variability was expected upon further follow up.

Upon further investigation, drug 24 (n=3) and 13 (n=5) did not significantly affect degranulation or killing (Figure 5.7B, D). Drug 26 (n=5, $p<0.01$, paired t-test, mean of differences = -13.25) and 30 (n=5, $p<0.05$, paired t-test, mean of differences = -11.35) significantly decreased degranulation to a small extent, but they did not have a significant effect on CTL killing (Figure 5.7E,F). The striking killing defect of drug 4 observed in the screen was not reproducible, however, CTL killing was decreased, at least to a small extent, in every experiment (n=7, Figure 5.7A). This possibly did not reach statistical significance due to the variability of the differences between DMSO and drug 4 treatment between repeats. Drug 19 was the only drug that reproducibly and significantly decreased degranulation (n=7, $p<0.01$, paired t-test, mean of differences = -40.41) and killing (n=7, $p<0.001$, paired t-test, mean of differences = -42.54) (Figure 5.7C).

The drug with the biggest effect size, drug 19, was investigated further. So far, drug 19 had only been tested with overnight treatment. I used the Incucyte killing assay, which measures the killing response over time, to test how quickly treatment with drug 19 resulted in a killing defect. In these assays hCTLs were not pre-treated with drug 19, instead the compound was only added at the start of the assay. This showed that drug 19 exerted its effect

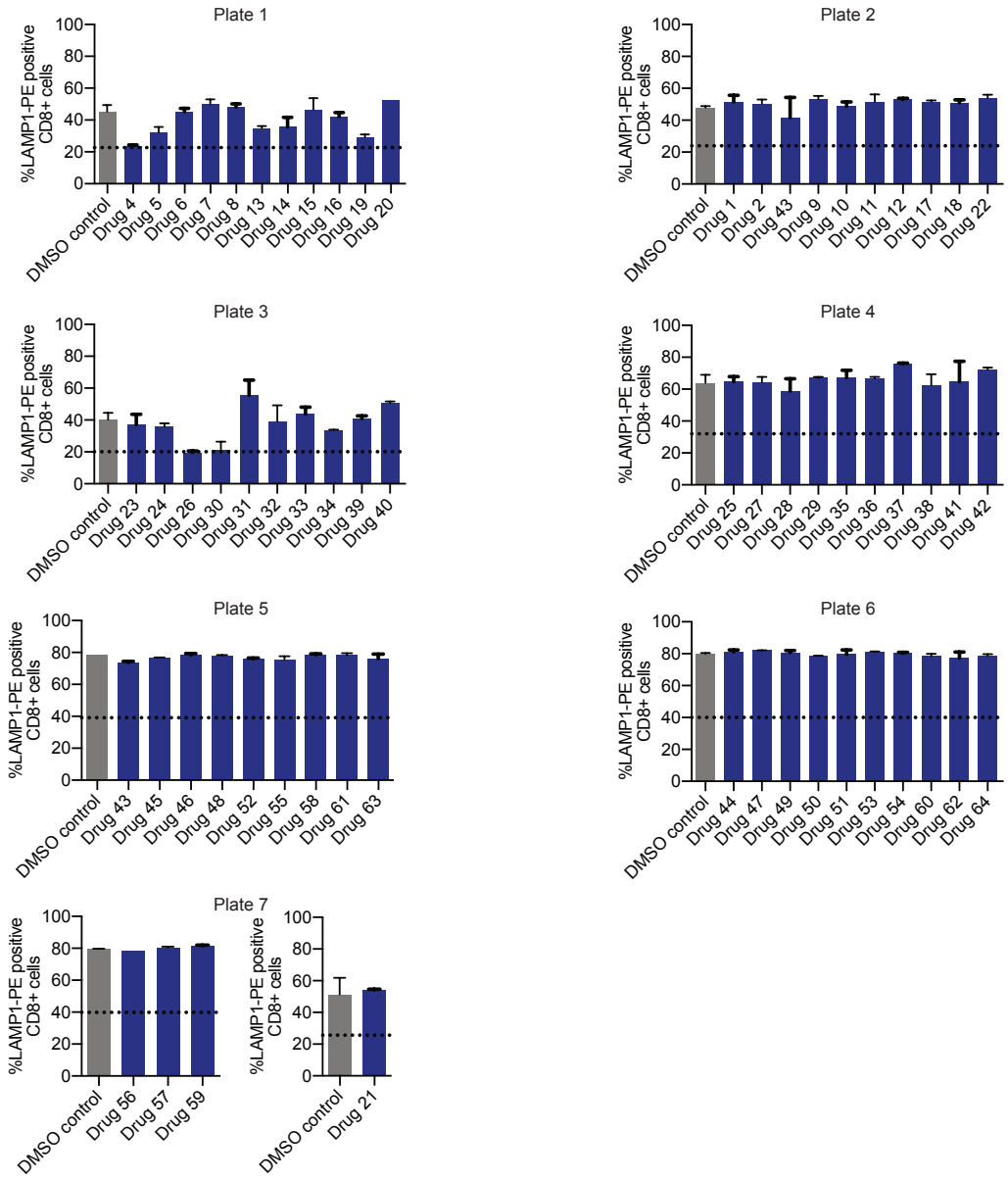

Fig. 5.5 ***Screening identified one drug that reduced degranulation by more than 50%.*** *Drugs were roughly grouped into plates according to their highest non-toxic concentration. A control containing the equivalent amount of DMSO to the highest concentration tested was included on every plate. CD8 cells from one HD were treated with compounds overnight. The following day, target cells with and without αCD3 were added. E:T ratio = 2.5:1, assay duration = 180 min. Technical duplicates were prepared for every condition, error bars represent the SD of technical repeats. Screening was performed in 7 plates across 3 days (2-3 plates per day). Degranulation assays were analysed following the gating strategy described in chapter 2, section 2.5.1 and 2.5.2. Drugs were classified as potential hits when the treatment decreased degranulation by more than 50% in comparison to the appropriate DMSO control. The dotted line indicates the 50% cut-off on each graph.*

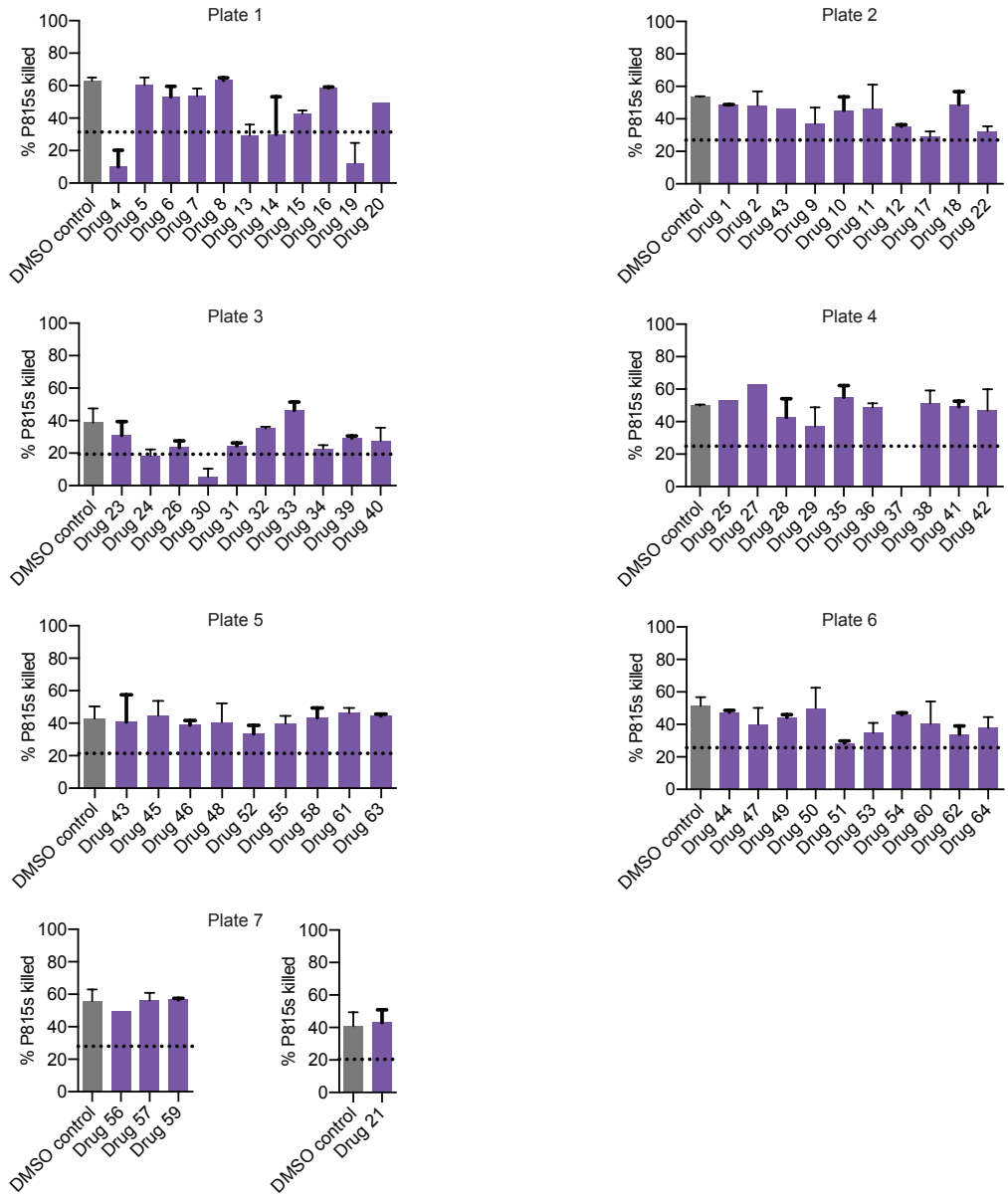

Fig. 5.6 ***Screening identified five drugs that reduced killing by more than 50%.*** *Drugs were roughly grouped into plates according to their highest non-toxic concentration. A control containing the equivalent amount of DMSO to the highest concentration tested was included on every plate. CD8 cells from one HD were treated with compounds overnight. The following day, target cells with and without αCD3 were added. E:T ratio = 2.5:1, assay duration = 180 min. Technical duplicates were prepared for every condition, error bars represent the SD of technical repeats. Screening was performed in 7 plates across 3 days (2-3 plates per day). Killing assays were analysed following the gating strategy and calculations described in chapter 2, section 2.5.2. Drugs were classified as potential hits when the treatment decreased killing by more than 50% in comparison to the appropriate DMSO control. The dotted line indicates the 50% cut-off on each graph. Drug 37 was excluded due to toxic effects on P815 target cells. SD = standard deviation.*

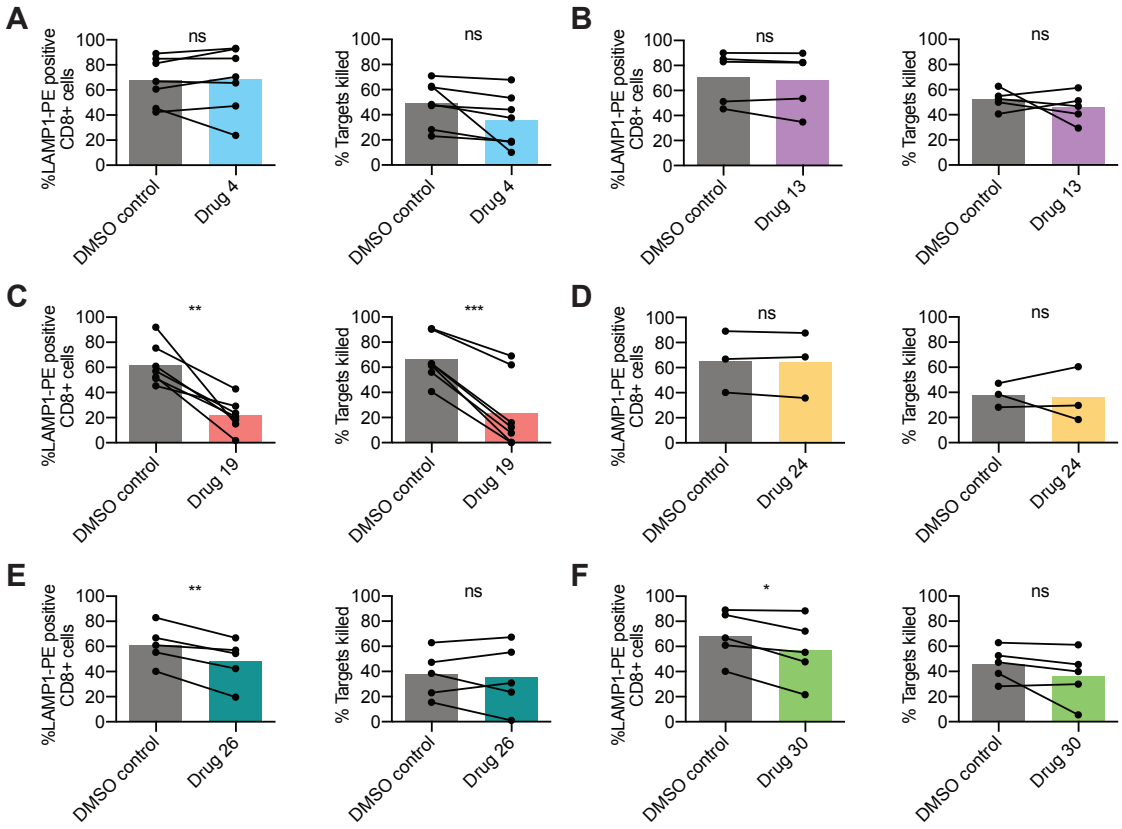

Fig. 5.7 ***Follow up of the effect of promising compounds on degranulation and killing.*** *Cells derived from independent HDs were treated overnight with drugs identified as potential hits in the screen. Each treatment is connected to its corresponding DMSO control. Each pair of data points represents an independent experiment. The combined degranulation and killing assay was analysed following the gating strategy and calculations described in chapter 2, section 2.5.2. E:T ratio = 2.5:1, assay duration = 180 min, each data point represents the average of technical duplicates. The following drugs were tested* ***A*** *drug 4 at 0.9 µM (n=7 independent experiments),* ***B*** *drug 13 at 8.3 µM (n=5 independent experiments),* ***C*** *drug 19 at 8.3 µM (n=7 independent experiments),* ***D*** *drug 24 at 0.9 µM (n=3 independent experiments),* ***E*** *drug 26 at 0.1 µM (n=5 independent experiments) and* ***F*** *drug 30 at 0.9 µM (n=5 independent experiments). *p<0.05, **p<0.01, ***P<0.001, calculated by paired t-test.*

on killing within the first hour (Figure 5.8A). Encouragingly, the killing defect observed with drug 19 treatment was also titratable in response to a two-fold (Figure 5.8B) and four-fold (Figure 5.8C) decrease in concentration.

A third kind of killing assay, the LDH release assay, was used to test the effect of drug 19 treatment when using a variety of E:T ratios (Figure 5.8D). Increasing the amount of effectors while keeping the amount of target cells constant resulted in an increase in the percentage of target cells killed over 3 h. The killing observed was significantly reduced in the presence of drug 19 across three different E:T ratios (n=4, p<0.001 for E:T 10:1, n=4, p<0.001 for E:T 5:1 and n=4, p<0.01 for E:T 2.5:1, paired t-test), further confirming the inhibitory effect of drug 19 on CTL killing.

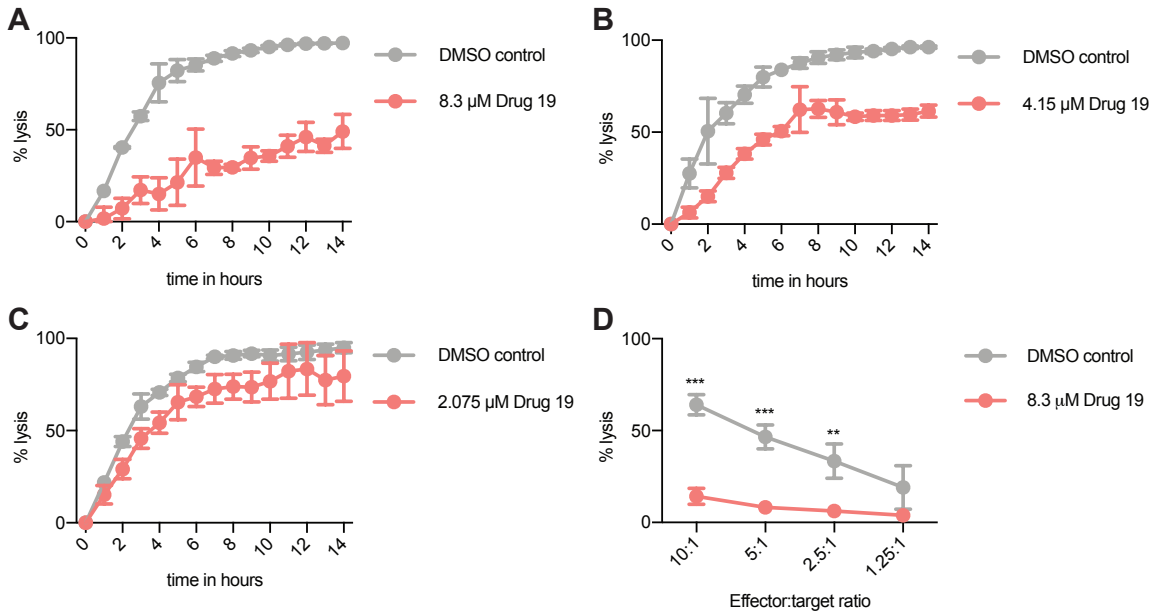

Fig. 5.8 ***Drug19 has an immediate effect on CTL killing.*** *Incucyte killing assays showing the percentage lysis of red P815 target cells over the course of 14 hours in the presence of αCD3, hCTL and drug 19 or equivalent DMSO vehicle control. One representative plot for 3 independent experiments is shown for using drug 19 at a concentration of* ***A*** *8.3 µM,* ***B*** *4.15 µM and* ***C*** *2.075 µM. E:T = 10:1. Each datapoint is an average of 3 technical repeats and the error bars show the SD.* ***D*** *LDH release killing assay showing the % lysis of P815 target cells at varying E:T ratios and in the presence of 8.3 µM drug 19 or equivalent DMSO vehicle control for 3 h, n=4 independent experiments for all E:T except E:T 1.25:1, where n=2 independent experiments. **p<0.01, ***P<0.001, calculated by paired t-test.*

5.2.5 The effect of drug 19 on NF-κB

Next, I tried to investigate at which point in the NF-κB activation cascade drug 19 intervenes in NF-κB signalling. Initially I used PMA and ionomycin stimulation in combination with drug 19 treatment. Studies have shown that PMA and ionomycin can be used to activate NF-κB in the absence of TCR, αCD3 or αCD28 stimulation (Liu et al., 2016). This treatment essentially bypasses TCR signalling and triggers degranulation. PMA activates PKCs, while ionomycin induces calcium release from the endoplasmic reticulum (Liu et al., 2016). I used PMA and ionomycin stimulation and measured surface exposure of LAMP1 in the presence and absence of drug 19 treatment. The fact that drug 19 treatment still reduced degranulation in response to PMA (n=5, $p<0.05$, paired t-test), ionomycin (n=5, $p<0.001$, paired t-test) and combined PMA and ionomycin (n=5, $p<0.01$, paired t-test) treatment suggested that the molecular target of drug 19 was not proximal to the TCR, but downstream of the molecular targets of PMA and ionomycin (Figure 5.9A).

To investigate whether drug 19 affected NF-κB transcription I measured the expression of the NF-κB target gene TNFα in the presence and absence of αCD3ε stimulation (Figure 5.9B). NF-κB p65/p50 heterodimers were shown to be involved in transcriptional activation of TNFα expression in response to LPS activation in macrophages (Liu et al., 2000). TNFα can therefore be used as a readout of p65/p50 transcriptional activity. TNFα was not produced in the absence of αCD3ε stimulation, independent of addition of DMSO or drug 19 (Figure 5.9B). Production of TNFα was upregulated in DMSO samples in response to αCD3ε stimulation for 4 h. This upregulation was significantly lowered in the presence of drug 19 (Figure 5.9B, n=3, $p<0.01$, paired t-test).

Using PMA and ionomycin treatment I investigated whether drug 19 affected phosphorylation of p65 at Ser536. Levels of phosphorylated p65 were increased in response to PMA and ionomycin treatment in the DMSO control (Figure 5.9C-D). This upregulation was decreased with drug 19 treatment (Figure 5.9C-D). Interestingly even basal levels of p65 phosphorylated at Ser536 seemed slightly lower in response to drug 19 treatment (Figure 5.9C-D). Taken together, these results suggest that drug 19 acts between PKC (Figure 5.9A) and p65 (Figure 5.9C-D) to potently inhibit p65-mediated transcription (Figure 5.9B).

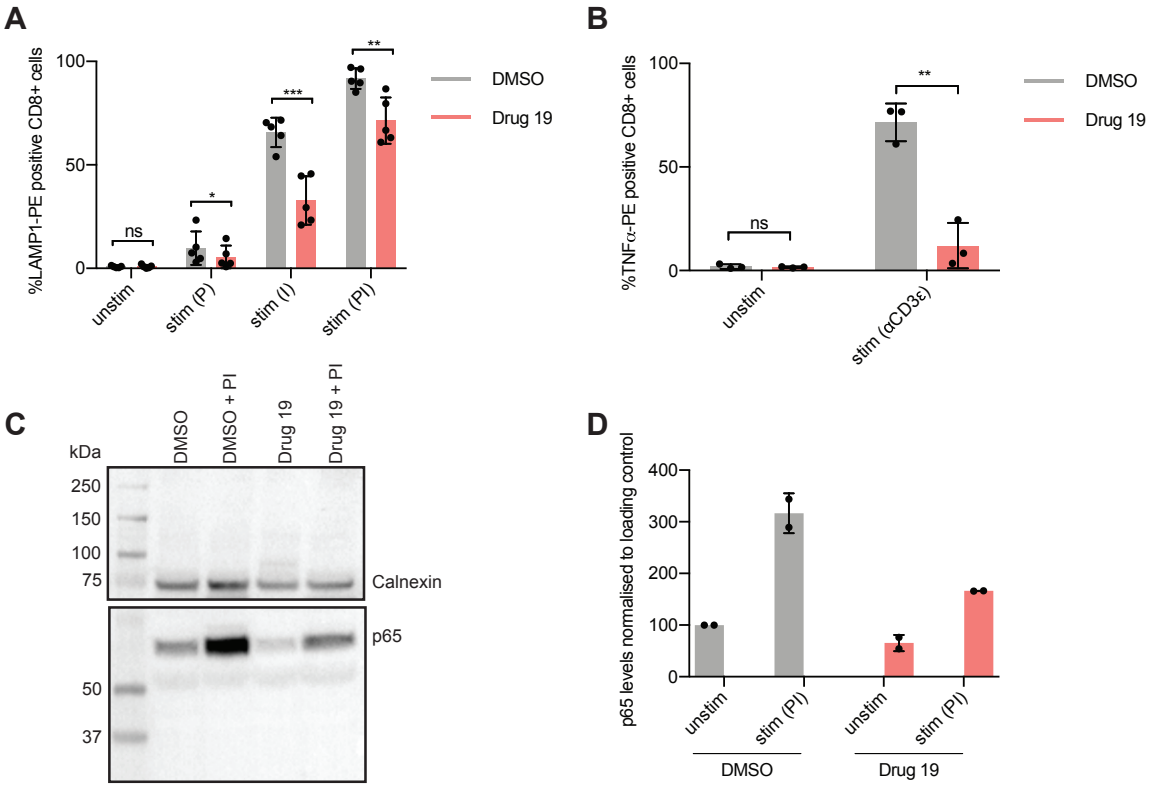

Fig. 5.9 ***Determination of the molecular effect of drug19 on NF-κB.*** ***A*** *Surface LAMP1 levels in response to treatment of hCTL with PMA (P), ionomycin (I), or both in the presence or absence of drug 19 for 3 h. The bar graphs show the average of 5 independent experiments, error bars show the SD, *p<0.05, **p<0.01, ***p<0.001 calculated by paired t-test.* ***B*** *TNFα expression in hCTL treated overnight with 8.3 µM drug 19 or DMSO followed by 4 h stimulation on αCD3-coated plates (stim) or uncoated plates (unstim control) was measured by intracellular FACS. The bar graphs show the average of 3 independent experiments, error bars show the SD, **p<0.01 calculated by paired t-test.* ***C*** *Representative WB showing p65 phosphorylated at Ser536 and calnexin (loading control) protein levels 4 h after treatment with PMA and ionomycin or appropriate DMSO vehicle control in addition to treatment with 8.3 µM drug 19 or DMSO vehicle control.* ***D*** *Average levels of p65 protein phosphorylated at Ser536 upon PMA and ionomycin treatment in the presence or absence of drug19 in 2 independent repeats. In each repeat p65 protein levels were expressed relative to the unstimulated control and normalised to calnexin. Bar graphs show the mean ± SD, n=2 independent experiments. P = PMA, I = ionomycin, unstim = unstimulated, stim = stimulated, ns = not significant, SD = standard deviation.*

5.3 Discussion

The combined degranulation and killing assay successfully detected phenotypes in hCTL derived from FHL2 and FHL3 patients (Figure 5.1A-B). The relatively mild killing phenotype observed with *MUNC13-4* patients in the Incucyte killing assay (Figure 5.1C-E) could be explained by only partial protein loss in these patients (Figure 5.1F). In patients with mutations in *PRF1* either no perforin protein was detected (patient 4166 and 392) or the perforin antibody recognised two bands of a higher MW (patient 6981 and 3026) than in the HDs (Figure 5.2G). Functional assays indicated that the higher MW versions of perforin were not functional (Figure 5.2A-F). Perforin undergoes various processing steps during its formation. First a ∼65 kDa version gets modified by glycans to give a 70 kDa version. Cleavage of the C-terminus yields the final functional 60 kDa version of perforin (Uellner et al., 1997). The final processing step did not seem to occur in patients 6981 and 3026, indicating that the domains affected by their mutations may be important for the C-terminal cleavage step. Uellner et al. (1997) reported that a mutant version of perforin, where the C-terminus is truncated, is located in the endoplasmic reticulum, rather than in lytic granules when expressed in RBL cells. It would therefore be interesting to test the localisation of perforin in CTL derived from patient 6981 and patient 3026 by immunofluorescence. In summary, the patient results confirmed that the combined degranulation and killing assay can be used in hCTL, and shows potential as a diagnostic test for patients suspected to have a CTL defect.

Next, the combined degranulation and killing assay was used to screen 64 compounds. To further improve the scalability of the assay, sample fixation to stably maintain the endpoint could be explored. Additionally it would be interesting to test the assay in a 384-well format, in order to be able to screen even more samples per plate while reducing the amount of cells and reagents needed per sample.

The drug screen identified 6 compounds that reduced degranulation or killing by more than 50% (Figures 5.5 and 5.6). There may be additional compounds in the library that affect degranulation or killing that were not identified due to using a suboptimal concentration, as I did not test concentrations above 25 μM. Additionally, the stringent 50% cut-off applied to the degranulation and killing readouts likely excluded some hits. For example, drug 19 was not picked up as an inhibitor of degranulation in the initial screen, as it did not decrease degranulation by more than 50% (Figure 5.5). However, drug 19 turned out to significantly decrease degranulation upon repetition (Figure 5.7). To avoid such false negatives, it would be preferable to perform screens in triplicates, as done for the genetic screen in chapter 4.

This would allow the identification of hits with greater certainty, however, the vast amount of time required to set up these assays limits the scale of such screens without a robot.

The most promising hit, drug 19, significantly reduced degranulation and killing after overnight treatment (Figure 5.7). A different kind of killing assay, the Incucyte assay, demonstrated that drug 19 already affected target cell killing within 1 h of treatment (Figure 5.8). Encouragingly, the effect of drug 19 was titratable when reducing the concentration by two-fold and four-fold, indicating that the effect on killing is mediated by the drug (Figure 5.8). I analysed distinct steps in the NF-κB activation cascade to determine where drug 19 mediated its effect. If the degranulation defect with drug 19 had been rescued with PMA and ionomycin treatment this would have suggested that drug 19 inhibits signalling proximal to the TCR. As this was not the case, drug 19 must act downstream of the molecular targets of PMA and ionomycin (Figure 5.9). TNFα transcription is known to be regulated by p65/p50 heterodimers (Liu et al., 2000). As TNFα production in response to αCD3ε stimulation was decreased in the presence of drug 19 (Figure 5.9), the effect of drug 19 on p65 was investigated. I found that drug 19 decreased the levels of p65 phosphorylated at Ser536 both in response to PMA and ionomycin treatment as well as at basal levels (Figure 5.9).

In the literature, parthenolide, the official name for drug 19, has been shown to directly bind to two components of the NF-κB cascade. It inhibits the ability of p65 to bind to DNA by alkylating cysteine-38 of p65 (Garcia-Pineres et al., 2001) and it inhibits IKKβ by alkylation of cysteine-179, leading to stabilisation of IκBα and IκBβ (Hehner et al., 1999; Kwok et al., 2001). In addition, other studies have shown that parthenolide also induced HDAC1 depletion (Gopal et al., 2007) and inhibits DNA methyltranferase 1 (Liu et al., 2009). With the data available in this chapter, I can therefore not be certain that the effect of parthenolide on CTL killing is due to its inhibition of NF-κB. This highlights a general disadvantage to using chemical compounds for screening, as they may affect multiple molecular targets, in contrast to a targeted genetic approach. The striking effect of parthenolide on CTL killing is nonetheless interesting, but how exactly the effect is mediated remains to be determined. Specifically targeting p65 by CRISPR or siRNA would help to clarify whether p65 is directly involved in CTL degranulation and killing. Furthermore, it would be interesting to investigate which steps in the killing pathway are affected by drug 19 treatment. The degranulation readout demonstrated that the lytic granule content is not secreted in response to drug 19 treatment. This could be due to a defect in fusion between the granule membrane and plasma membrane, or due to a block at an earlier step in the CTL killing process. Immunofluorescent microscopy could be used to determine whether treated CTLs can still form contacts with

target cells and whether the centrosome and lytic granules still polarise towards the contact site.

Several other studies have suggested parthenolide as a potential cancer treating drug (reviewed by Ghantous et al. (2013)). A recent study noted anti-proliferative and pro-apoptotic effects of parthenolide in glioma cells, and showed that parthenolide inhibits tumour growth in mice (Yu et al., 2018). For such medical purposes, it is crucial to be aware of the suppressive effect that parthenolide has on CTL killing.

In its current format, the combined degranulation and killing assay can be used to screen many dozens of compounds over the course of several days. It is therefore a useful tool to screen compounds as well as genetic targets. Furthermore, the experiments with patient-derived CTL demonstrated the potential of the assay as a diagnostic test. Using patient derived NK cells and CTLs in a simple degranulation assay has already been proposed as a tool for diagnostic evaluation of patients presenting with FHL symptoms (Bryceson et al., 2012; Chiang et al., 2013). However, it has been noted that this approach requires additional monitoring of perforin expression in all clinical samples, as the defect resulting from mutations in *PRF1* cannot be detected using the degranulation assay (Bryceson et al., 2012). The combined degranulation and killing assay presented in this thesis therefore provides an advantage over the current gold standard. By cutting out the requirement of analysing perforin separately the assay reduces time, effort and the amount of patient material required for diagnosis.

5.3.1 Summary and evaluation of aims

- Test the combined degranulation and killing assay in hCTL using FHL2 and FHL3 patient samples.
  - The assay was successfully validated using patient-derived samples. The defects caused by *PRF1* mutations would not have been picked up by the simple degranulation assay, which is currently being used for diagnostic purposes. The combined assay that is able to detect both degranulation and killing simultaneously could therefore have great diagnostic potential.
- Investigate the scalability of the assay using the NF-κB compound library.
  - 64 compounds were screened in technical duplicates across 3 days using CD8 T cells derived from one HD. Out of the drugs tested, 1 drug decreased degranulation

and 5 drugs decreased killing by more than 50 % in the screen. These promising hits were followed up using CTL derived from independent HDs. The most promising compound, drug 19 (parthenolide), reproducibly decreased CTL degranulation (n=7, $p<0.01$, paired t-test) and killing (n=7, $p<0.001$, paired t-test).

- Follow up promising hits to elucidate their mechanism of action.
  - Measuring CTL killing over time revealed that parthenolide reduced CTL killing within the first hour of treatment. The effect of parthenolide on NF-κB in primary human T cells was tested at various steps along the NF-κB activation cascade. Parthenolide treatment was shown to suppress phosphorylation of p65 at Ser536 and decreased TNFα gene expression in response to αCD3ε stimulation, indicating potent inhibition of gene transcription that is regulated by p65.